City Research Online

City, University of London Institutional Repository

This is the accepted version of the paper.

This version of the publication may differ from the final published version.

Quadrotor Multibody Modelling by VehicleSim: Adaptive Technique for Oscillations in a PVA Control System

Silvia Estelles. M Tomas-Rodriguez.
School of Engineering and Mathematical Sciences, City University London, London, UK.

Abstract

The work presented here covers the detailed modelling and trajectory control for an elastic bladed quadrotor vehicle. The benefits of using VehicleSim modelling software are also discussed. The authors present a full elastic structural and dynamical model as well as two different aerodynamic models. These two aerodynamic models differ from each other on their level of complexity and therefore, accuracy. The control methodology employed to stabilize and guide the vehicle is PVA (Proportional-Velocity-Acceleration), derived and implemented by using Simulink. As it will be shown, it stabilises and provides satisfactory quadrotor trajectory tracking.

Since the control methodology feeds back the acceleration of the vehicle, and this acceleration has an oscillating nature, an adaptive process has been designed and introduced into the vehicle's model in order to avoid the oscillations' transmission to the control system, showing how it reduces the amplitude of the control actions oscillations.

Results of simulations and discussion on them are also provided at the end of this article.

Keywords

VehicleSim, quadrotor, translational speed modelling, oscillations.

I. Introduction

The use of quadrotor vehicles has increased considerably in the last years due to the large number of possible applications. This kind of vehicles presents numerous advantages in high risk missions, with high manoeuvrability requirements and reduced vehicle's dimensions. These vehicles present vertical take-off, landing and hover capabilities, which convert the vehicle in a suitable device for good performance in reduced spaces.

Due to the increasing applications of the quadrotors, especially in sensitive environments and missions, the accuracy in their performance needs to be guaranteed at all times.

The project in which this work is embedded searches for a more accurate and stable quadrotor platform by reducing the vibrations produced by the rotary elements. In order to accomplish this goal, a complete structural and aerodynamic model has been derived by VehicleSim for the first time, a software that obtains the complete equations of motion from the vehicle's configuration description.

The model, stabilised and controlled with a control system designed with Simulink, will be used in the next step of the project in order to characterize and isolate the vibrations introduced by the rotating blades.

II. Modelling and simulation tool

The software used in this work is VehicleSim (VehicleSim, 2014), a modelling and rigid multibody simulation software. This software has been used previously by members of this research group in modelling and control of various vehicle systems such as motorcycles (Ramirez et al., 2012, 2013), (Ramirez and Tomás-Rodríguez, 2014), and helicopters (Marichal et al., 2012, 2014). Its old version, Autosim allowed the modelling of several mechanical system in a similar manner to the work here presented (Evangelou et al., 2008,

2012), (Tomás-Rodríguez and Sharp, 2007). The software has proven to be adequate to obtain nonlinear models by (Limebeer and Sharp, 2006) and (Evangelou et al., 2006). VehicleSim consists of a group of LISP macros which allow the description of mechanical systems integrated by several bodies, with the possible addition of non-mechanical systems. It allows the development of complex models through multibody methodology. VehicleSim consists of two independent but correlated programs; VS-Lisp and VS-Browser.

In VS-Lisp, each body is considered as a rigid body and it is defined by its degrees of freedom (rotation and translation), mass and inertia matrix and by its relation to other bodies. It is also necessary to define the forces and moments applied to each body. Using the advanced formulation of Kane's equations (Kourosh, 2007), and applying algebraic and computational optimization methods, the software obtains the equations of motion from the model's physical description.

On the other hand, VS-Lisp solves the differential equations' system, and the output can take three different formats: 1) an .rtf text file, which contains the symbolic equations of the described system; 2) a C file containing the model parameters and the simulation control commands; or 3) a Matlab file containing the equations of system's motion and the states' matrices A, B, C and D very convenient for linear analysis and control purposes.

Once the model has been built up and compiled, the resultant file is independent from VehicleSim and it can be executed as many times as needed, without modelling or compiling again the system, even in the case the state variables' initial conditions change.

Despite the great offer of available programming software, VehicleSim is used due to the advantages it presents: representation of complex systems composed by different bodies and non-mechanical devices, quantification of the interaction between these bodies, lineal

and nonlinear equations' derivation, fast numerical solution of these equations and compatibility between this software and other platforms specialized in simulation and control like Simulink, which has been used to carry out the control system's implementation in this work.

VehicleSim modelling software, VS-Lisp.

At first, the modelling process consists on the environment definition: units system, choice of linear or nonlinear equations' derivation and force fields' definition. VS-Lisp provides different predefined units system (`si`, `mks`) and also allows to define or change the units in a specific units system. In this work the International System of units has been used, including also the degree units for angular position.

An inertial reference system, n, is added automatically to all models which has a fixed origin point n_0, and three associated perpendicular directions [X_n, Y_n, Z_n]. Based on this inertial reference frame, the bodies that conform the model are added sequentially, indicating their physical properties (mass, inertia, gravity centre, etc.) and their degrees of freedom with respect to the parent (translations and rotations). Each body has an associated local Cartesian coordinate system, which their 'child's'' coordinates are expressed in. This local coordinate system is defined by: 1) a reference system which the coordinate system is associated to; 2) an origin point; and 3) three mutually orthogonal directions that define the local axes. An example of the coordinate systems associated to each body in a multibody system developed in VS-Lisp is shown in Figure 1.
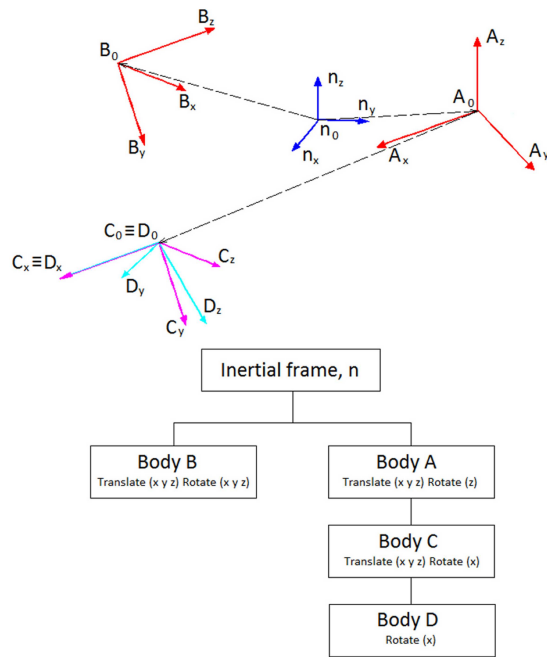
Figure 1. Example of Cartesian coordinate systems associated to different bodies in VS-Lisp and their parent-child structure.

Besides their degrees of freedom and restrictions, each body has some other characteristic parameters. These are represented by the symbol of the parameter with a subscript indicating the body it is referred to, so the mass of a body named E is M_E, the position of its mass centre is MC_E and so on.

The definition of one body in VS-Lisp is shown below, which in this case corresponds to the main quadrotor's structure:

```
(add-body :name "str"
   :parent n
   :joint-coordinates n0
```

```
:mass "Mstr"

:cm-coordinates (cmx cmy cmz)

:translate (x y z)

:inertia-matrix (Ix Iy Iz)

:body-rotation-axes (z y x)

:parent-rotation-axiz z

:reference-axis [nx])
```

Once the structural layout is completely defined and the restrictions between bodies are established, the external forces and moments acting on the system should be included in the model. In the case under study in here, these forces and moments will be the aerodynamic forces and control moments.

As in the bodies' description, the definition of the aerodynamic forces and moments is shown below:

```
(add-line-force Lij

  :name "liftij"

  :direction [Siz]

  :magnitude @Lij

  :point1 cp0

  :body1 Bij)

(add-moment MDi

  :name "MDi"

  :direction [Siz]

  :magnitude @MDi

  :body1 Si
```

```
:body2 n)
```
For each of these forces and moments, the direction, magnitude and body of action is stated.

III. Quadrotor dynamic and aerodynamic behaviour

Quadrotors are vehicles whose propulsion and elevation are provided by the action of four equispaced rotors distributed around a central structure. The propulsion is created by the blades' angle of attack and the angular rotation around a central hub. Trajectory tracking is achieved by means of the angular speed change of one or more rotors, leading to a change on the propulsion on each of them and generating in this way a force imbalance which produces the vehicle's displacement. The control systems and electronic sensors are usually hosted in the centre of the vehicle structure and are used to stabilise the quadrotor (Hoffmann et al., 2004).

Quadrotor performance description.

The main forces governing quadrotors behaviour are the weight, W, and the aerodynamic forces acting on the blades (lift, L and drag, D) and on the structure (translational drag, TD). These are represented in Figure 2.
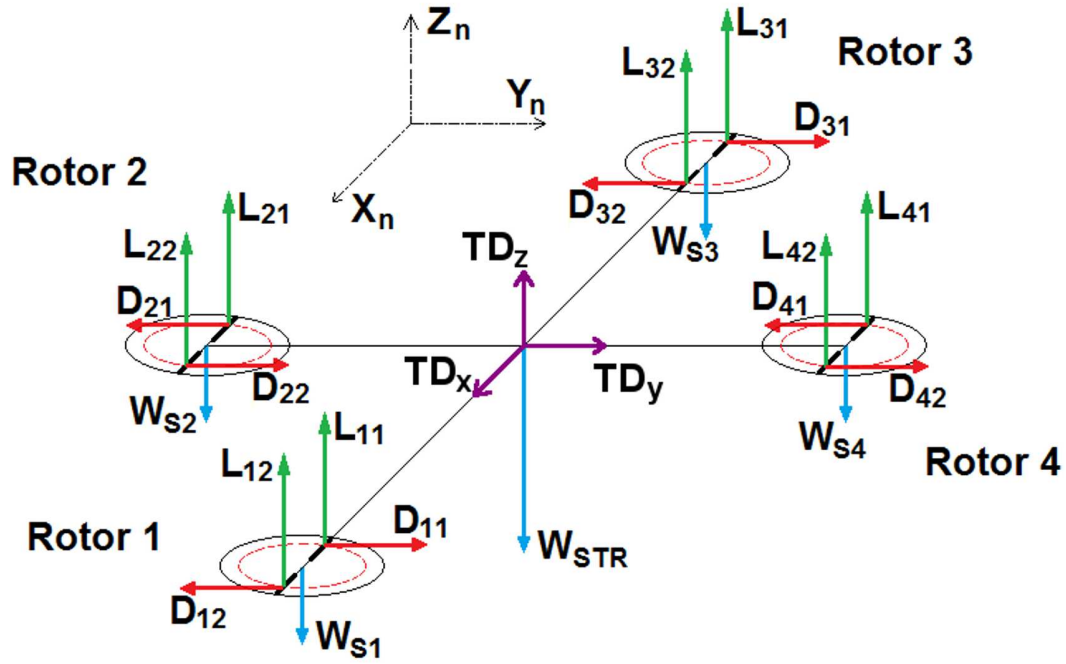
Figure 2. Representative diagram of two-bladed rotors' and blades' position around the central body. Lift (L), drag (D), translational drag (TD) and weight (W) forces are indicated.

The resultant forces of the weight, W, act at the mass centre of each element and point downwards towards the ground (W_{S1}, W_{S2}, W_{S3}, W_{S4} and W_{STR} in Figure 2). Since the vehicle is considered symmetric, the translational drag (TD) is supposed to act at the centre of the structure and is proportional to the linear speed of it (Park et al. 2005), (Patel et al, 2012), through a drag coefficient which usually has values between 0.0005 Ns/m and 0.01 Ns/m (Bouadi et al, 2011), (Salih et al, 2010) for quadrotors of similar dimensions. The aerodynamic force acting on the blades is provided by the pressure and shear distributions over the object's surface, both of them appear due to the relative displacement between the

object and the surrounding airflow. The total effect of these distributions integrated along the blade surface is the aerodynamic resultant force applied at the pressure centre. This force can be divided into two components: lift and drag forces:

Lift (L): It is the component of the aerodynamic force that is perpendicular to the direction defined by the relative movement of the blade with respect to the airflow (L_{11}, L_{12}, L_{21} ... in Figure 2).

Drag (D): It is the component of the aerodynamic force that is parallel to the direction defined by the relative movement between the blade and the airflow. This force opposes the blade motion on the rotor disk (D_{11}, D_{12}, D_{21} ... in Figure 2).

The aerodynamic forces are given by the following expressions:

$$L = \frac{1}{2}\rho_\infty S C_L(\alpha) V_\infty^2 \quad (1)$$

$$D = \frac{1}{2}\rho_\infty S C_D(\alpha) V_\infty^2 \quad (2)$$

ρ_∞ is the air's density, S is a constant reference surface, V_∞ is the relative speed between the blade and the airflow and $C_L(\alpha)$ and $C_D(\alpha)$ are the lift and drag coefficients respectively, which are mainly dependent on the angle of attack, α, between the airflow and the chord of the blade, as seen in expressions (3) and (4), where C_{L0} represents the Lift Coefficient at zero angle of attack, $C_{L\alpha}$ is the slope of the Lift Coefficient-Angle of Attack curve and cd represents the profile drag coefficient obtained from the Prandtl's Lifting-Line Theory (Anderson JDJ, 2001).

$$C_L(\alpha) = C_{L_0} + C_{L_\alpha}\alpha \quad (3)$$

$$C_D(\alpha) = c_d + kC_L^2 \quad (4)$$

The values of the parameters in expressions (3) and (4) were obtained in (Estelles S, 2013). For the type of rotary-wing vehicles consisting on four rotors rotating in opposite directions (rotors 1 and 3 in Figure 2 rotate counter-clockwise whilst rotors 2 and 4 rotate clockwise), there are four control variables. The control variables considered in this work are the moments applied from the stator to the motor and are modelled as moments acting from the structure to the rotors.

The displacement of the vehicle is achieved by varying the moments applied to each rotor, so that the rotational speeds of the rotors are varied in this way, different aerodynamic forces are obtained, and the imbalance of these forces around the different axes associated to the structure generates the system's acceleration.

In Figure 3 the vehicle's degrees of freedom are shown: three rotational (roll $\phi(t)$, pitch $\theta(t)$ and yaw $\psi(t)$) and three translational (longitudinal $x(t)$, lateral $y(t)$ and vertical $z(t)$). The quadrotor's structure has six degrees of freedom and only counts with four control inputs (moments applied to each rotor), therefore some variables must be related to each other: lateral and longitudinal translations will be determined by the horizontal component of the lift force, which is related to the total lift force by means of the quadrotor orientation with respect to the inertial reference system.
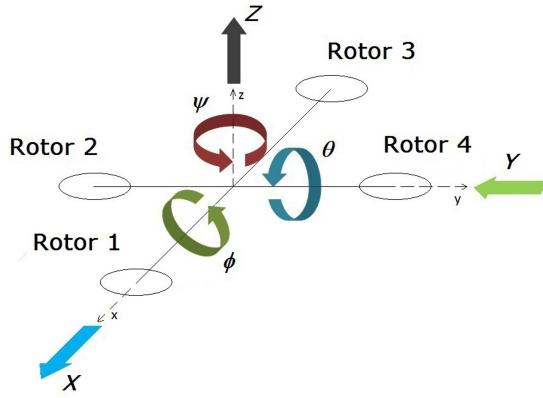
Figure 3. Representative diagram of the structure's degrees of freedom: roll $\phi(t)$, pitch $\theta(t)$, yaw $\psi(t)$, longitudinal $x(t)$, lateral $y(t)$ and vertical $z(t)$.

IV. Structural model

This section describes the system in detail, pointing out the various bodies that conform the vehicle, their respective degrees of freedom and properties. Figure 4 is a representative diagram of the quadrotor bodies' distribution and Figure 5 shows the parental structure followed in the multibody system's definition.
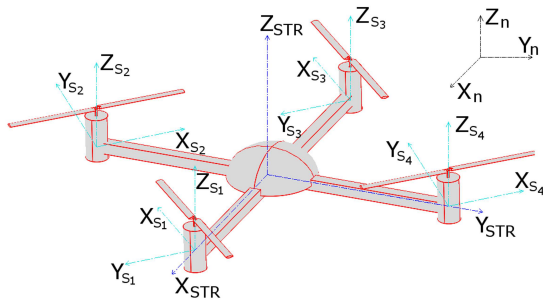

Figure 4. Representative sketch of quadrotor bodies' distribution and the structure's and rotors' associated axes.
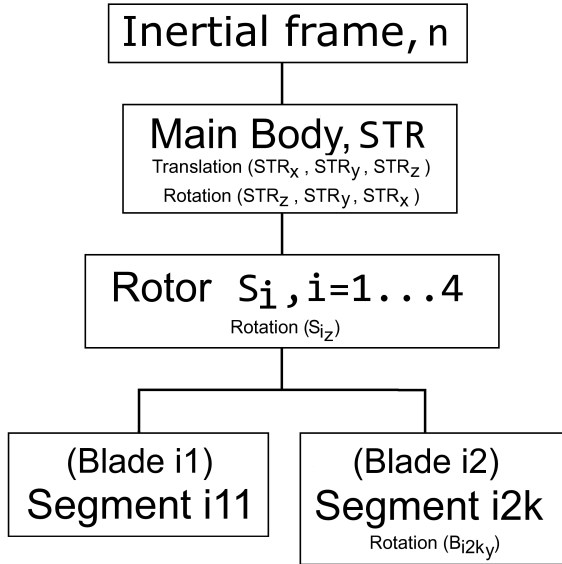
Figure 5. VehicleSim parent-child structure defining the quadrotor as a multibody system, with blade `i1` considered rigid and blade `i2` considered elastic, discretized in k segments with rotation allowed around B_{i2ky} axis.

Quadrotors are usually composed by two equal arms in a cross shape, whose intersection hosts the batteries, the electronic control circuit, the IMU sensor and the devices needed for the adequate performance of the vehicle. All these elements, the arms and the electronic devices, have been modelled in this work as a lumped rigid body, `STR`. The main body is defined at the inertial reference system, `n`, with six degrees of freedom with respect to it, with no restriction, so `STR`'s motion is only governed by the forces and moments' imbalance around the $[X_{STR}, Y_{STR}, Z_{STR}]$ axes.

One rotor is placed at each arm's end, the model has a total of four rotors. Each rotor is identified by S_i, ($i=1,...,4$), and they are allowed one degree of freedom; rotation around their corresponding local Z axis, Z_{Si}.

There are two opposite blades attached to each rotor i, B_{ij} ($j=1,2$), which depending on the structural model, are considered rigid or elastic. The subscript i is used to identify the rotor's number, the subscript j identifies the corresponding blade on the ith rotor, and the subscript k identifies the segment of the blade when considered elastic.

In this work, only untwisted blades are considered with a constant symmetric airfoil along the span. It leads to a constant structural angle of attack along the span, α_s.

In the rigid structural model, the blades do not have any degree of freedom with respect to the rotor. As for the rotor elastic model, the blades are considered to have the flap degree of freedom, since due to the dimensions of the blade, lag and torsional movements are less likely to occur.

In order to model the elastic blades with a rigid multibody software, they have been discretized in three segments; a shorter segment close to the root with no motion allowed, and two double length segments with one degree of freedom around their respective Y_{ijk} axis, flap motion. The motion of the two free segments is constricted by a restoring moment, which is modelled as a rotational spring and a damper that can reproduce the static and dynamic properties of a specific material.

The constant of the rotational springs has been found to respond to expression (5), where E represents the elasticity modulus of the material, I is the second moment of inertia of the blade's cross section, R is the blade length, n_t is que equivalent total number of segments if they were considered of the same length -5 in this case-, and n_f is the equivalent number of segments free to move if they were considered of the same length -4 in this case. With this

value for the constant of the rotational spring, the maximum deflection of the discretized blade equals the maximum deflection of the continuous blade, and also a good agreement of the first and second natural frequencies is obtained with what is expected from Beam Theory (Venkatesan, 2014).

$$b_n = \frac{3EI}{R}\left(\frac{1}{2} + \frac{1/2}{n_t}\right)\frac{n_f}{n_t} \quad (5)$$

As for the damper constant, it has been chosen in such a way that the decay of the flap motion in the discretized blade model matches the hysteretic damped motion of the continuous blade made of an specific material, which is given by expression (6) (Orban, 2011), where A is the amplitude of the tip motion, A_o is the initial displacement from the equilibrium point, ξ is the damping ratio of the material and ω_n is the first natural frequency of the continuous blade.

$$A = A_o e^{-2\pi\xi\omega_n t} \quad (6)$$

The material selected for the blades is the ABS plastic, widely used for the manufacture of quadrotor blades, and also the most elastic one, so the effects of the elastic blades consideration can be well appreciated. Thus, considering a value for the elastic modulus of 1.5GPa, which is a sensible value in between the usual range (Ashby, 2005), and a damping ratio of 0.0975 obtained as an average value from different samples measured (Dundar, 2012), the spring and damper parameters for the ABS plastic with the discretization already explained are b_n = 0.0865 Nm/rad and c_n = 0.0009 Nms/rad.

Once the structural model is completely defined, external forces and moments are applied, which in this model are the aerodynamic forces governing the vehicle's performance, calculated in Section V, and the control moments, calculated in Section VI.

V. Aerodynamic models

In this section an overview for the aerodynamic forces model is given; what they consist on, how they act on the vehicle, different existing modelling approaches and how they have been modelled in this work.

As it was explained in Section III, the total aerodynamic load acting on a blade can be divided in two components: lift force, L, and drag force, D. Different authors have modelled these forces in various ways: neglecting the translational velocity when compared to the rotational velocity (Alexis et al., 2012), considering the lift force to be applied at the shaft centre (Erginer and Altug, 2007), modelling the drag forces as moments around the shaft axis (McKerrow, 2004), considering the variation of total thrust in translational flight (Hoffmann et al., 2007), considering blade flapping effects on lift and drag forces (Bristeau et al., 2009) ...etc.

As the final aim of this research is to reduce the vibrations produced by the rotary parts of the quadrotor, a simple aerodynamic model is not appropriate since it does not reflect the complexity of the aerodynamics involved in the quadrotor's performance. For that reason, two different aerodynamic models have been implemented, starting from a simplest one and increasing its complexity afterwards.

The first model consists on a simplified aerodynamic model which neglects the effect of the translational speed on the lift and drag forces and has been used to design the control system. The second model considers the contribution of the quadrotor's translational speed

to the aerodynamic forces' calculus and the relative angle of attack between the airflow and the chord blade, and this second model has been applied to both, the rigid and the elastic structural models.

Both of them are described in this section and the simulations' results carried out with these models will be presented in Section VIII.

For all the models considered, the aerodynamic drag forces have been modelled as moments around the vertical axis of each of the rotors (7), as it is shown in Figure 6.

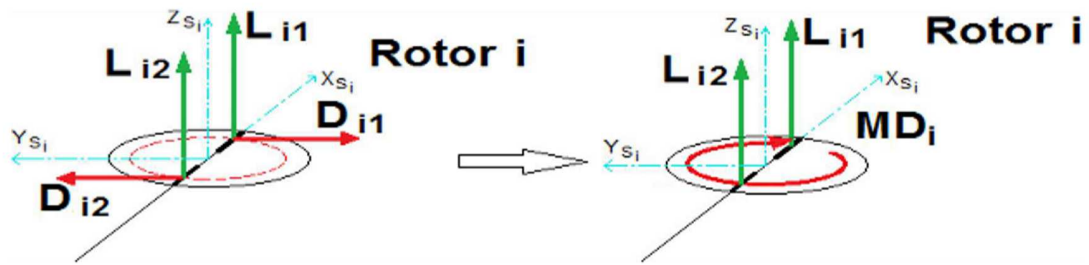$$MD_i = \sum_{j=1}^{2} D_{ij} r_{cp_j} \quad (7)$$

Figure 6. Equivalence between drag forces, Di, and drag moment, MDi, acting on the rotor.

Aerodynamic forces as a function of rotational speed.

The most common aerodynamic model for control purposes in quadrotors considers the aerodynamic forces as a function of the rotational speed and various fixed parameters (Alexis et al., 2012), (Erginer and Altug, 2007). This is the simplest aerodynamic model, used in this work to design the control system.

The lift forces and drag moments produced by the rotors for non-translational speed can be modelled as follows:

$$L_{ij}(\alpha_j) = \frac{1}{2}\rho_\infty S C_L(\alpha_j)\left[r_{rep_0}\Omega_i\right]^2 \quad (8)$$

$$MD_i(\alpha_j) = -\frac{1}{2}\rho_\infty S \sum_{j=1}^{2}(-1)^{i+1} C_D(\alpha_j)r_{cp_0}\left[r_{rep_0}\Omega_i\right]^2 \quad (9)$$

Ω_i is the rotational speed of rotor i, r_{rep_0} is the position of the representative point of the blade in stationary conditions, which is located in such a position on the blade that considering a uniform distribution of its corresponding lift force along the blade length is equal to the lift force obtained by considering a variable lift distribution dependent on the speed of the different sections forming the blade (Estelles, 2013: 66-68) and r_{cp_0} is the pressure centre of the blade calculated in stationary conditions, where the resultant aerodynamic forces act (Estelles, 2013: 68-70).

Both drag moments and lift forces are calculated considering the stationary values of the representative point, r_{rep_0}, and have been placed at the stationary values of the pressure centre, r_{cp_0}, as these points remain fixed during the simulation. This provides a simpler model which has been used to develop the initial control system design.

The drag moment reduces the rotational speed of the rotor and there is a need to compensate it in order to keep the adequate rotational velocity. This will be taken into account during the control design process presented in Section VI.

Aerodynamic forces as a function of rotational and translational speed.

Once the control system is designed, implemented and validated for different manoeuvres considering the previous aerodynamic model, a further level of complexity is added,

achieving in this way a more realistic model: The variation of the aerodynamic forces and the angle of attack with translation is considered.

The equations of the complete aerodynamic model now are:

$$L_{ij}(\alpha_j) = \frac{1}{2}\rho_\infty SC_L(\alpha_j)\left[V_t + r_{rep_j}\Omega_i\right]^2 \quad (10)$$

$$MD_i(\alpha_j) = -\frac{1}{2}\rho_\infty S \sum_{j=1}^{2}(-1)^{i+1} C_D(\alpha_j)r_{cp_j}\left[V_t + r_{rep_j}\Omega_i\right]^2 \quad (11)$$

Where V_t represents the speed the blade experiences as a result of the motion of the vehicle and r_{rep_j} is the actual value of the representative point of blade j. Both lift force and drag moment are applied at the aerodynamic pressure centre of each blade, r_{cp_j}, which is not constant in this model.

In the previous aerodynamic model the angle of attack was considered constant (α_s) since the effect of the translation was not considered. In this more complete model, the translation is taken into account, affecting the angle of attack as shown in (12).

$$\alpha_j = \alpha_s + \alpha_i \quad (12)$$

Where α_i represents the incidence angle of the airflow with respect to the disk plane as seen in Figure 7.
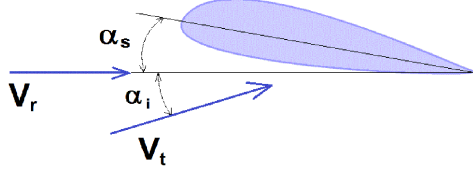
Figure 7. Relative velocities and incidence's angles of attack in a cambered airfoil considered in the aerodynamic forces modelling.

In this way, by including the variation of the aerodynamic forces and angle of attack with the translational speed a more complete and realistic model is obtained.

Aerodynamic model as a function of rotational and translational speed for elastic blades. The previous section explained the aerodynamic forces applied to rigid blades. In order to simulate a flexible blade, the blade is discretized in more than one segment, the aerodynamic forces are now calculated for each of these segments as function of the rotational and translational speed and applied at their respective pressure centre. Assuming constant lift and drag coefficients along the span, the lift forces and drag moments for each segment are now as follows:

$$L_{ijk}(\alpha_j) = \frac{1}{2}\rho_\infty S_k C_L(\alpha_j)\left[V_{t_j} + r_{rep_{ijk}}\Omega_i\right]^2 \quad (13)$$

$$MD_i(\alpha_j) = -\frac{1}{2}\rho_\infty(-1)^{i+1}\sum_{k=1}^{n}\left(S_k \sum_{j=1}^{2} C_D(\alpha_j)r_{cp_{ijk}}\left[V_{t_j} + r_{rep_{ijk}}\Omega_i\right]^2\right) \quad (14)$$

S_k is the representative surface of the segment k, $r_{rep_{ijk}}$ is the representative point of segment k in blade j, and the forces are applied at the pressure centre of each segment, $r_{cp_{ijk}}$.

VI. Control System Design.

The control system implementation has been carried out using the Simulink platform (Mathworks, 2014). This software is widely used both in modelling electrical devices (Le-Huy, 2001), electronic devices (Karden et al., 2002), (Ropp and Gonzales, 2009), and mechanical devices (Hajjaji and Ouladsine, 2001), control design and simulation (Altas and Sharaf, 2007) and in real-time control (Pivonka and Miksnek, 2007), just to cite a few. It is also used in sensors and predictors implementation (Qiu et al., 2004). Besides, the interaction between the control system implemented in Simulink and the VehicleSim's dynamic model is available in real-time, being this a very good advantage.

The control of the quadrotor is achieved by varying the rotational speed of the rotors as the aerodynamic forces depend on the blades' squared speed and the rotation is the main contribution to the velocity. In order to modify the rotor's rotational speed, a moment needs to be applied from the structure. This moment changes the angular acceleration, increasing or decreasing in this way, the rotational speed of the rotors.

To simplify the control design process, the rigid simple aerodynamic model with aerodynamic forces as function of rotational speed only ((8)-(9)) has been used and afterwards, once the control methodology is designed, it has been applied to the system when the more complex aerodynamic models were implemented; the rigid complete model ((10)-(11)) and the elastic complete model ((13)-(14)).

Control moments' definition.

The control methodology designed to stabilise and control the quadrotor's trajectory is the PVA (Position-Velocity-Acceleration) methodology. The standard PVA control consists

on the application of a control action that is proportional to the position error, $e_p(t)$, the velocity error, $e_v(t)$, and the acceleration error, $e_a(t)$, through the control parameters k_1, k_2 and k_3 respectively:

$$u(t) = [k_1 \quad k_2 \quad k_3][e_p(t) \quad e_v(t) \quad e_a(t)]^T \quad (15)$$

This methodology has been selected from a large choice of options due to the following reasons:

This particular method is widely used in the control of positioning devices in which the overshoot needs to be suppressed (Ning and Bone, 2002).
One of the most interesting features of this methodology is the advantage in computational load it represents, which is considerably lighter than other more sophisticated methods. It leads to a faster control action.

The control actions for the quadrotor's manoeuvring are the moments the electrical motors generate and apply to each rotor. These moments are divided in different components depending on the variable they are intending to control:

Height control, $z_{STR}(t)$. The moments applied to each rotor for the height control are of equal magnitude, therefore they produce the same angular speed variation in the four rotors and consequently, the same lift variation. The only special consideration is made according to the different direction of rotation of the rotors; moments applied to rotors 1 and 3 are positive and moments applied to rotors 2 and 4 are negative.

$$CM_{i_z} = (-1)^{i+1}\left[k_{1_z}\left(z_{STR}^{ref} - z_{STR}\right) + k_{2_z}\left(\dot{z}_{STR}^{ref} - \dot{z}_{STR}\right) + k_{3_z}\left(\ddot{z}_{STR}^{ref} - \ddot{z}_{STR}\right)\right] \quad (16)$$

Roll control, $\phi_{STR}(t)$. The control moments for the vehicle's roll are only applied to rotors 2 and 4 since this degree of freedom is mainly governed by these rotors.

$$CM_{2_\phi} = \left[k_{1_\phi}\left(\phi_{STR}^{ref} - \phi_{STR}\right) + k_{2_\phi}\left(\dot{\phi}_{STR}^{ref} - \dot{\phi}_{STR}\right) + k_{3_\phi}\left(\ddot{\phi}_{STR}^{ref} - \ddot{\phi}_{STR}\right)\right] \quad (17)$$

$$CM_{4_\phi} = -\frac{|\Omega_2|}{\sqrt{\frac{mg}{\rho C_L r_{rep_0}^2} - \Omega_2^2}} CM_{2_\phi} \quad (18)$$

Pitch control, $\theta_{STR}(t)$. As in the roll control case, the pitch dynamics are mainly governed by two rotors; therefore, the control moments are applied to rotors 1 and 3.

$$CM_{3_\theta} = \left[k_{1_\theta}\left(\theta_{STR}^{ref} - \theta_{STR}\right) + k_{2_\theta}\left(\dot{\theta}_{STR}^{ref} - \dot{\theta}_{STR}\right) + k_{3_\theta}\left(\ddot{\theta}_{STR}^{ref} - \ddot{\theta}_{STR}\right)\right] \quad (19)$$

$$CM_{1_\theta} = -\frac{|\Omega_3|}{\sqrt{\frac{mg}{\rho C_L r_{rep_0}^2} - \Omega_3^2}} CM_{3_\theta} \quad (20)$$

Yaw control, $\psi_{STR}(t)$. In order to keep the moments balance around the X_{STR} and Y_{STR} axes constant, the moments applied to opposite rotors should be of equal magnitude; in this way, the roll and pitch moment are cancelled.

$$CM_{1,3_\psi} = \left[k_{1_\psi}\left(\psi_{STR}^{ref} - \psi_{STR}\right) + k_{2_\psi}\left(\dot{\psi}_{STR}^{ref} - \dot{\psi}_{STR}\right) + k_{3_\psi}\left(\ddot{\psi}_{STR}^{ref} - \ddot{\psi}_{STR}\right)\right] \quad (21)$$

$$CM_{2,4_\psi} = -\frac{|\Omega_{1,3}|}{\sqrt{\frac{mg}{\rho C_L r_{rep_0}^2} - \Omega_{1,3}^2}} CM_{1,3_\psi} \quad (22)$$

The expressions (18), (20) and (22) have been calculated such that the roll, pitch and yaw control actions do not interfere with the vertical displacement, z_STR(t); i.e. the total lift remains constant (Estelles, 2013: 70-72).

As it was mentioned in Section III, the lateral and longitudinal vehicle's positions (y_STR(t), x_STR(t)) are determined by the structure's inclination (ϕ_STR(t), θ_STR(t)) and the total lift (L). In order to take this interaction into account, lateral and longitudinal references have been included in the roll and pitch references, and it is shown in the following:

$$\phi_{STR}^{ref} = -\left[k_{1_y}\left(y_{STR}^{ref} - y_{STR}\right) + k_{2_y}\left(\dot{y}_{STR}^{ref} - \dot{y}_{STR}\right) + k_{3_y}\left(\ddot{y}_{STR}^{ref} - \ddot{y}_{STR}\right)\right] \quad (23)$$

$$\theta_{STR}^{ref} = -\left[k_{1_x}\left(x_{STR}^{ref} - x_{STR}\right) + k_{2_x}\left(\dot{x}_{STR}^{ref} - \dot{x}_{STR}\right) + k_{3_x}\left(\ddot{x}_{STR}^{ref} - \ddot{x}_{STR}\right)\right] \quad (24)$$

$$\dot{\phi}_{STR}^{ref} = -\left[k_{d1_y}\left(\dot{y}_{STR}^{ref} - \dot{y}_{STR}\right) + k_{d2_y}\left(\ddot{y}_{STR}^{ref} - \ddot{y}_{STR}\right) + k_{d3_y}\left(\dddot{y}_{STR}^{ref} - \dddot{y}_{STR}\right)\right] \quad (25)$$

$$\dot{\theta}_{STR}^{ref} = -\left[k_{d1_x}\left(\dot{x}_{STR}^{ref} - \dot{x}_{STR}\right) + k_{d2_x}\left(\ddot{x}_{STR}^{ref} - \ddot{x}_{STR}\right) + k_{d3_x}\left(\dddot{x}_{STR}^{ref} - \dddot{x}_{STR}\right)\right] \quad (26)$$

$$\ddot{\phi}_{STR}^{ref} = -\left[k_{dd1_y}\left(\ddot{y}_{STR}^{ref} - \ddot{y}_{STR}\right) + k_{dd2_y}\left(\dddot{y}_{STR}^{ref} - \dddot{y}_{STR}\right) + k_{dd3_y}\left(y^{iv}{}_{STR}^{ref} - y^{iv}{}_{STR}\right)\right] \quad (27)$$

$$\ddot{\theta}_{STR}^{ref} = -\left[k_{dd1_x}\left(\ddot{x}_{STR}^{ref} - \ddot{x}_{STR}\right) + k_{dd2_x}\left(\dddot{x}_{STR}^{ref} - \dddot{x}_{STR}\right) + k_{dd3_x}\left(x^{iv}{}_{STR}^{ref} - x^{iv}{}_{STR}\right)\right] \quad (28)$$

Now, roll and pitch profiles can be calculated and they provide the desired lateral and longitudinal positioning.

The values of the control parameters, k's, used in the simulations are shown in Table 1.

Table 1. Control parameters' values.

Parameter	Value	Parameter	Value
$k_{1\theta}$	0.5	$k_{1\phi}$	0.5
$k_{2\theta}$	0.3	$k_{2\phi}$	0.3
$k_{3\theta}$	0.01	$k_{3\phi}$	0.01
$k_{1\psi}$	0.08	k_{1z}	0.1
$k_{2\psi}$	0.1	k_{2z}	0.1
$k_{3\psi}$	0.001	k_{3z}	0.11
k_{1x}	0.005	k_{1y}	0.005
k_{2x}	0.18	k_{2y}	0.18
k_{3x}	0.12	k_{3y}	0.12
k_{d1x}	4	k_{d1y}	4
k_{d2x}	0.1	k_{d2y}	0.1
k_{d3x}	0.0	k_{d3y}	0.0
k_{dd1x}	0.0	k_{dd1y}	0.0
k_{dd2x}	0.0	k_{dd2y}	0.0
k_{dd3x}	0.0	k_{dd3y}	0.0

Thus, the total control moment applied to each rotor is the addition of the moments derived to control each variable and the counter drag moment to be explained in next section:

$$CM_1 = CM_{1_z} + CM_{1_\theta} + CM_{1_\psi} + CDM_1 \quad (29)$$

$$CM_2 = CM_{2_z} + CM_{2_\phi} + CM_{2_\psi} + CDM_2 \quad (30)$$

$$CM_3 = CM_{3_z} + CM_{3_\theta} + CM_{3_\psi} + CDM_3 \quad (31)$$

$$CM_4 = CM_{4_z} + CM_{4_\phi} + CM_{4_\psi} + CDM_4 \quad (32)$$

Counter drag moment, CDM_i

The drag forces have been modelled as moments applied from the air to the rotors, resulting in rotational speed slowdown. In order to reduce the effect of these moments in the quadrotor behaviour and control, an additional term needs to be added to the control actions in order to counteract the drag moments; this is the counter drag moment.

The counter drag moment is opposite to the aerodynamic drag moment and, depending on the model it is applied to, it may have different expressions although all of them are based on the stationary flight rotational speed, Ω_0.

In the counter drag moment's calculations, the stationary flight rotational speed, Ω_0, is used instead of the real rotational speed of each shaft, Ω_i, in order not to cancel completely the effect of drag in the dynamical behaviour of the quadrotor and to introduce in the model the uncertainty usually present in the drag characterization. In this way, the control system demonstrates its robustness to uncertainties in the drag characterization.

The counter drag moment helps to reduce the effect of the drag moment due to the rotational speed of the rotor. It acts even when there is no displacement, in order to maintain the hover speed of the rotors, Ω_0. This implies that even for hover there will always be a torque acting on the rotors, CDM_0.

A standard rule for quadrotors design is that the combined lift forces must generate around the double of the hover lift force, meaning that hovering conditions should be achieved at 50% of maximum thrust. Based in this rule, and considering that the counter drag moment

in hover conditions for the quadrotor modelled here is $CDM_0 = 0.0561$ Nm, the maximum torque allowed will be $CM_{max} = 0.11$ Nm, which would mean that the CDM_0 represents 51% of the maximum torque.

Counter drag moment as a function of rotational speed.

The drag moment on each shaft can be modelled as a function of the angle of attack and the rotational speed, as expressed in (9). Therefore, the counter drag moment for each rotor has a similar but opposite expression:

$$CDM_i(\alpha_j) = \frac{1}{2}\rho_\infty S \sum_{j=1}^{2}(-1)^{i+1} C_D(\alpha_j) r_{cp_0} \left[r_{rep_0} \Omega_0 \right]^2 \quad (33)$$

Counter drag moment as a function of rotational and translational speed.

In this case, the counter drag moments have been calculated similarly to the previous one, making use of the stationary flight rotational speed and including the translational speed, V_t, too in this case.

For the aerodynamic model considering the translational speed, the drag moment is represented by (11). Therefore the counter drag moments can be expressed as:

$$CDM_i(\alpha_j) = \frac{1}{2}\rho_\infty S \sum_{j=1}^{2}(-1)^{i+1} C_D(\alpha_j) r_{cp_j} \left[V_t + r_{rep_j}\Omega_0 \right]^2 \quad (34)$$

The application of the counter drag moment leads to a reduction of the drag moment effect on the shafts' rotational speed, helping in this way to maintain the rotational speed of the rotors.

Counter drag moment for elastic blades

The counter drag moment when elastic blades are considered needs to be calculated for each of the various blade segments of the blade and applied as a single moment acting around the Z_{si} axis of the rotor.

$$CDM_i(\alpha_j) = \frac{1}{2}\rho_\infty(-1)^{i+1}\sum_{k=1}^{n}\left(S_k\sum_{j=1}^{2}C_D(\alpha_j)r_{cp_{ijk}}\left[V_{t_j} + r_{rep_{ijk}}\Omega_0\right]^2\right) \quad (35)$$

Smooth predefined trajectories

In most trajectory and guidance control applications, the reference signals represent the desired position that the vehicle should reach. One of the most common reference signal is the step input. Taking into account that the control law is proportional to the position error, $e_p(t)$, a step reference implies a high and abrupt initial control action, therefore different control parameters are needed to stabilise the quadrotor response when different amplitudes of steps' references are applied in order not to saturate the control actions: The larger the reference amplitude, the smaller the values of the parameters needed. This leads to a slow response of the vehicle for high values of the references. However, by defining smooth reference signals, the vehicle's response improves in time and positioning, as shown in Figure 8.
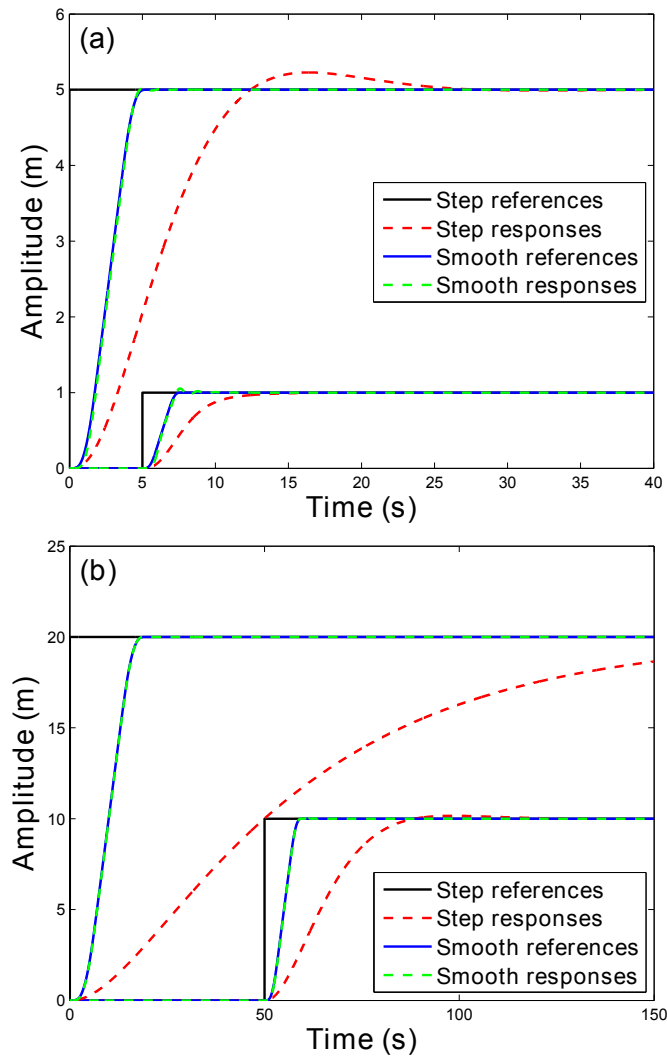
Figure 8. Comparison of responses to step and smooth reference signals for different longitudinal displacements on the X_n axis. (a) 1 and 5 meters translation, (b) 10 and 20 meters translation.
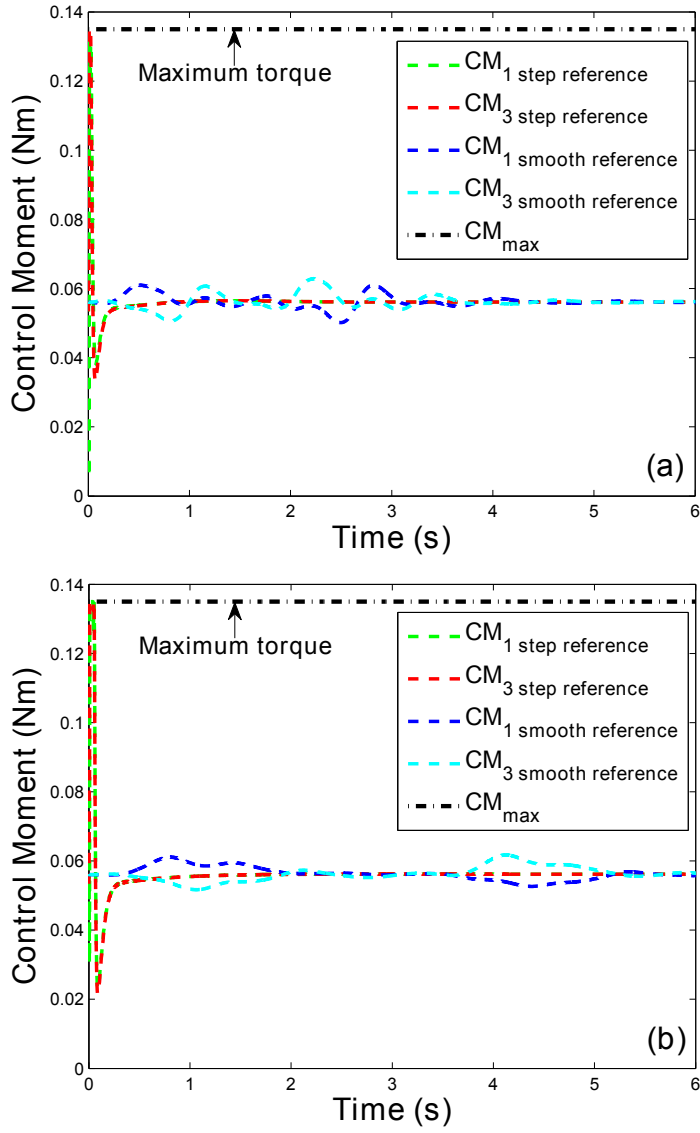
Figure 9. Control actions applied for 1 meter and 5 meters longitudinal displacement, comparing step reference and smooth reference inputs for the rigid simple model.

Figure 9 represents the control actions necessary for the rigid simple model to follow some of the trajectories shown in Figure 8. It can be seen that when step references are applied to the vehicle, the control actions present an initial high peak due to the instantaneous error of position that produces control action saturation. However, for smooth predefined trajectories, the position error is not instantaneous, therefore the control actions are smoother and far from reaching the saturation limits.

The use of smooth trajectories as reference signals has several advantages; constant control parameters for the indirectly controlled variables instead of variable functions, the possibility to define the maximum acceleration and speed values and smaller and smoother control actions; all these lead towards a better performance of the quadrotor, minimizing the presence of vibrations introduced by the control system so the structural vibrations produced by the mobile components of the system can be analysed.

Fifth order trajectories have been chosen in this research. It implies quadratic curves for the acceleration derivative, third order curves for the acceleration, fourth order curves for the speed and fifth order curves for the position reference signals, as shown in Figure 10.
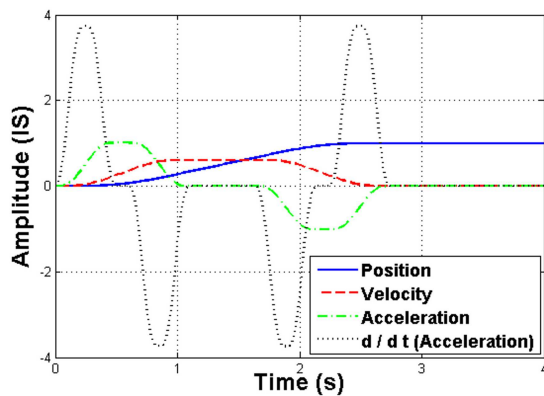

Figure 10. Fifth order trajectory signals example generated by Matlab and applied to the quadrotor.

VII. Adaptive process applied to the complete aerodynamic model.

Once the control system and the smooth predefined trajectories have been designed, they are applied to the complete aerodynamic model in order to validate its performance.

As the complete model also considers the translational speed, the aerodynamic forces have now an oscillating nature; they vary according to the blade's angular position in the plane disk, increasing when the blade is advancing and decreasing when the blade is retreating.

These oscillations in the forces imply oscillations also in the accelerations of the structure around its axis, mainly in roll and pitch accelerations.

These oscillations, due to the different speeds observed by the two blades in the same rotor, appear even in the rigid structural model ((10)-(11)) and their effect is slightly increased when elastic blades are considered ((13)-(14)), as can be seen in Figure 11 for pitch acceleration when a longitudinal displacement of 1 meter is considered.
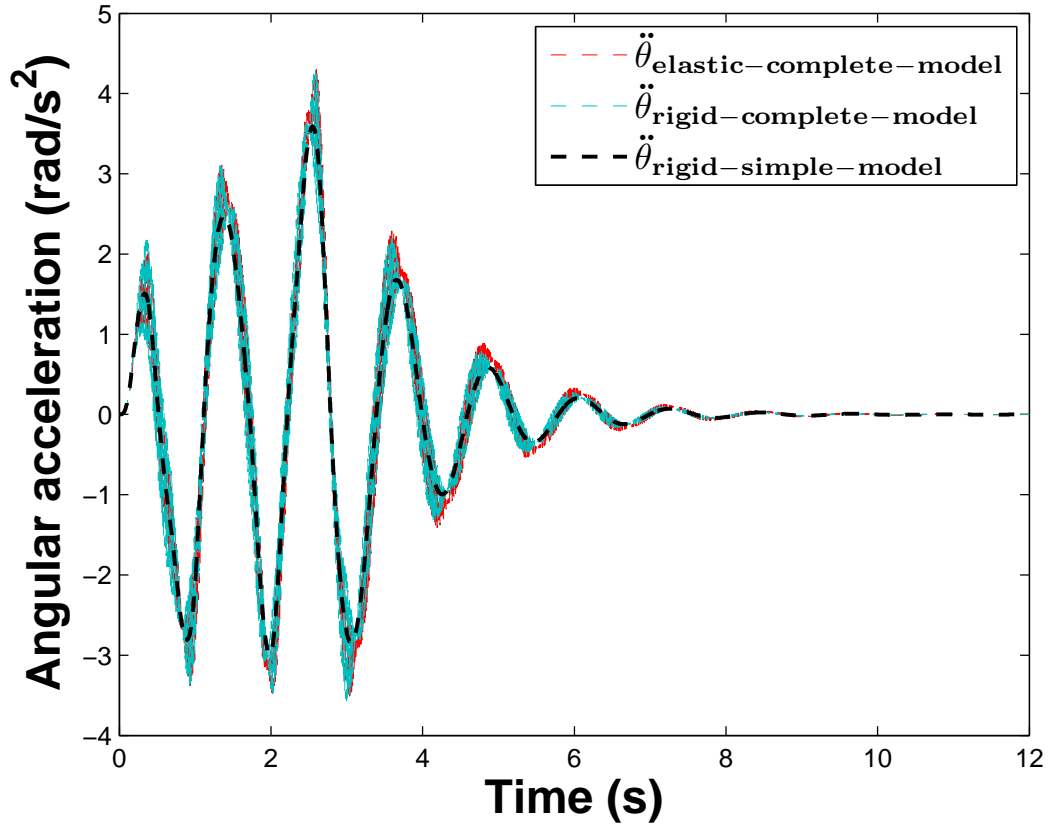
Figure 11. Pitch acceleration corresponding to a 1 meter longitudinal displacement. Elastic complete aerodynamic model (red), rigid complete aerodynamic model (blue) and rigid simple aerodynamic model (black).

Since the difference between the elastic and rigid aerodynamic models is small -regarding the oscillations transmitted to the structure-, only the analysis with the elastic model will be considered from now on.

The oscillations appearing in the roll and pitch accelerations are a consequence of the oscillation in the lift forces; however, as the control actions depend on the acceleration of

the structure, those oscillations will be transmitted to the moments applied to the rotors, increasing and decreasing the rotational speed at the rotational frequency (see Figure 12).
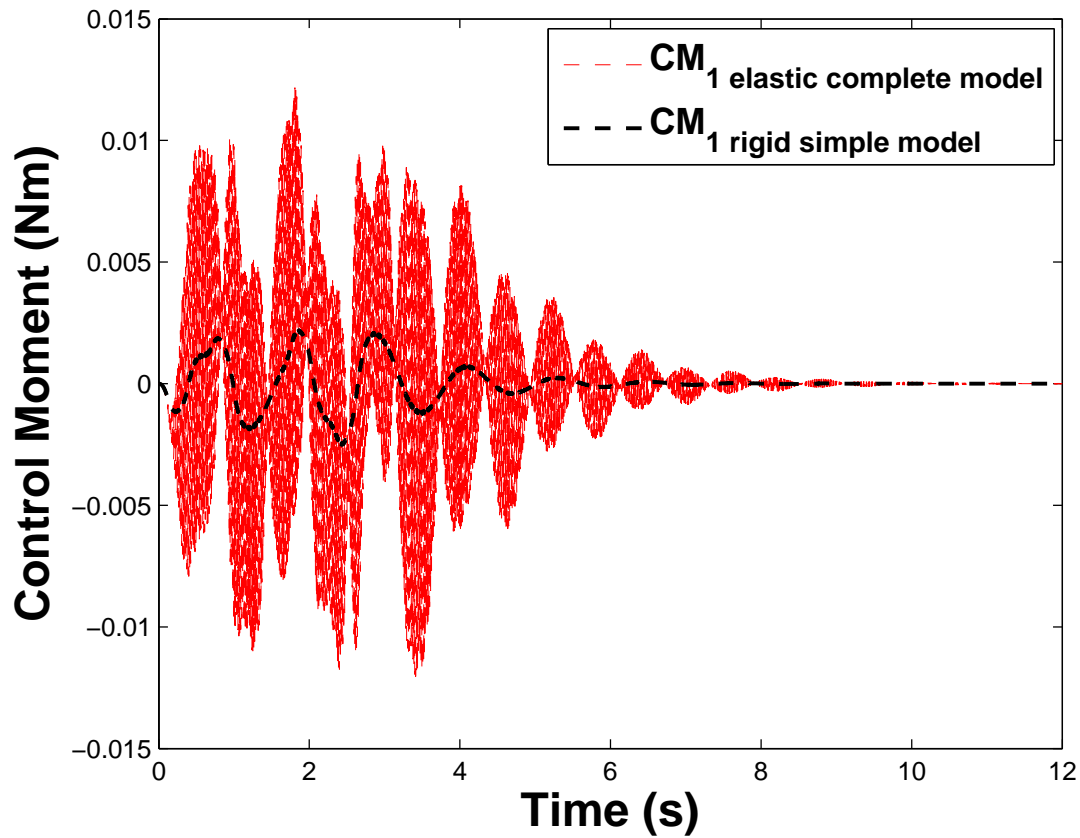

Figure 12. Control actions corresponding to rotor 1 for 1 meter longitudinal displacement. Elastic complete aerodynamic model (red) and rigid simple aerodynamic model (black). The appearance of oscillations in the control actions could cause destabilisation in the vehicle's performance, therefore it exits the need to reduce the oscillations in the control moments. For this purpose, an adaptive process has been designed.

Based on the comparison of the accelerations of the different aerodynamic models (elastic complete and rigid simple) for one particular choice of trajectory, a corrected acceleration is calculated. It has an intermediate value between the one corresponding to the elastic complete (oscillating) and the rigid simple simulation's acceleration, depending on the amplitude on the position error and an established tolerance.

An example of the corrected acceleration compared to the simple and complete aerodynamic models' acceleration is shown in Figure 13.
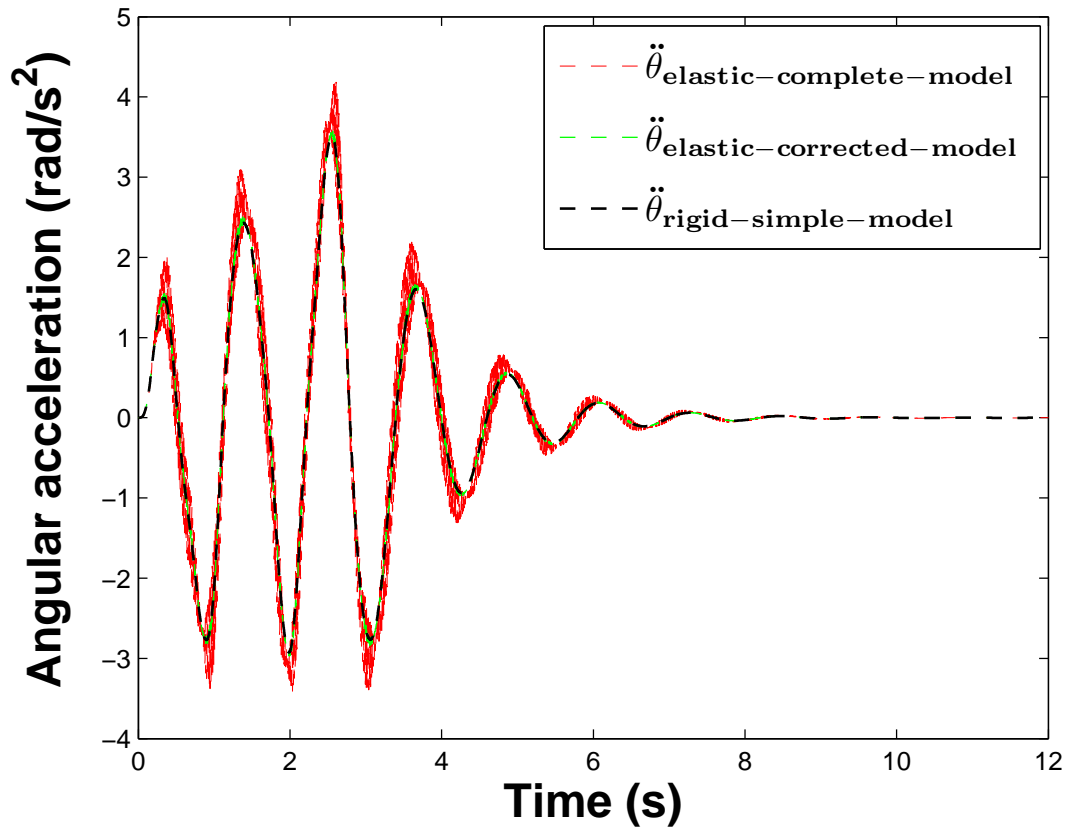
Figure 13. Pitch accelerations corresponding to 1 meter longitudinal displacement for different aerodynamic models: elastic complete aerodynamic model (red), elastic corrected model (green) and rigid simple model (black).

The corrected acceleration is then used to calculate the control action, as shown in (36).

$$CM_{3_\theta} = \left[k_{1_\theta}\left(\theta_{STR}^{ref} - \theta_{STR}\right) + k_{2_\theta}\left(\dot{\theta}_{STR}^{ref} - \dot{\theta}_{STR}\right) + k_{3_\theta}\left(\ddot{\theta}_{STR}^{ref} - \ddot{\theta}_{CORR}\right)\right] \ (36)$$

The amplitude of the oscillations of the control moment is reduced (see Figure 14), leading to the same trajectory produced by that one using the complete unaltered acceleration.
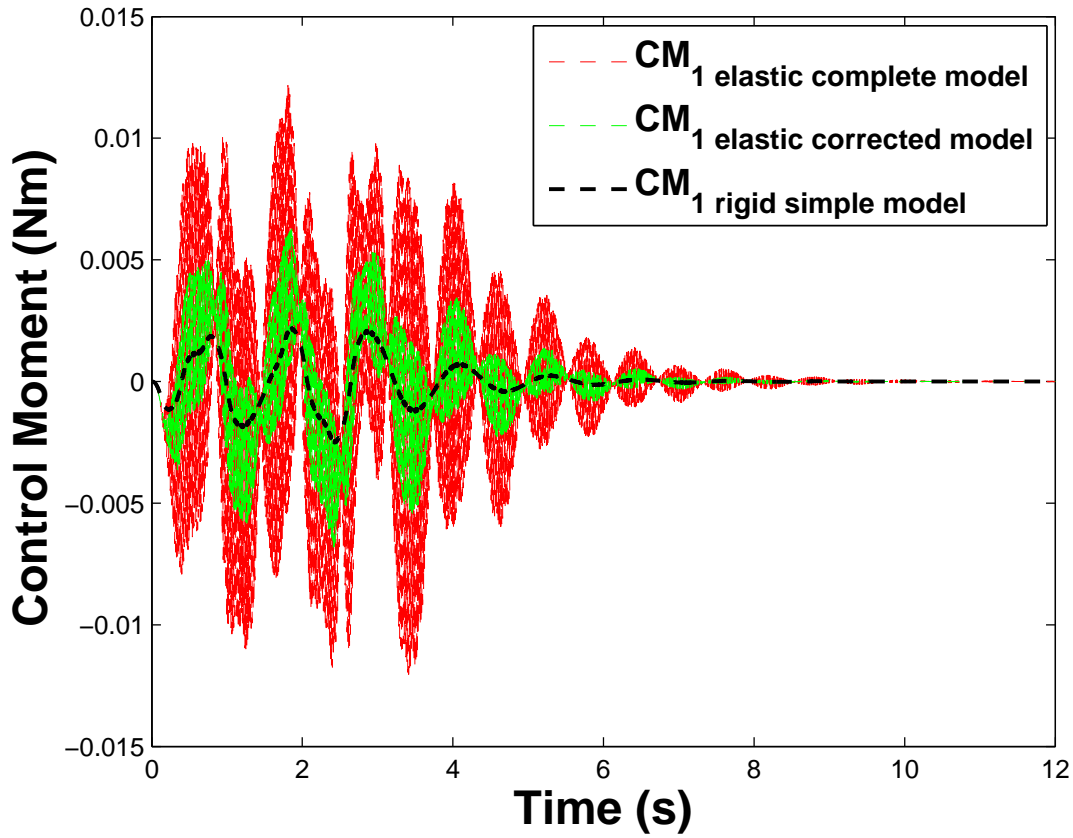
Figure 14. Comparison between the control actions that lead to 1 meter longitudinal displacement. Elastic complete model (red), elastic corrected model (green) and rigid simple model (black).

The adaptive technique is successful in correcting the value of the acceleration in the control process, and could be used in the speed if necessary, reducing oscillations introduced into the control system by the complex aerodynamics involved in a quadrotor's behaviour.

VIII. Results

In this section the main results obtained from simulations of the previous presented models are presented and discussed. This includes:

The mathematical model that represents the structural model described in Section IV.
The main simulations carried out with the elastic structural model and the different aerodynamic models developed in Section V.
The control system described in Sections VI and VII is applied.
And the control actions that lead to satisfactory trajectory tracking.

Mathematical model

The motion equations have been obtained from the VehicleSim generated text file and written down according to the terminology used in this work. These equations represent the acceleration of the corresponding degrees of freedom for the complete model:

$$\ddot{X} = g \sin \phi + \dot{\psi}\dot{Y} - \dot{\theta}\dot{Z} - \frac{TD_x}{M_{STR} + \Sigma_{i=1}^4 M_{S_i}} \ (37)$$

$$\ddot{Y} = -g \sin \theta \cos \phi - \dot{\psi}\dot{X} + \dot{\phi}\dot{Z} - \frac{TD_y}{M_{STR} + \Sigma_{i=1}^4 M_{S_i}} \ (38)$$

$$\ddot{Z} = -g \cos \theta \cos \phi - \dot{\phi}\dot{Y} + \dot{\theta}\dot{X} + \frac{L - TD_z}{M_{STR} + \Sigma_{i=1}^4 M_{S_i}} \ (39)$$

$$\ddot{\phi} = \frac{1}{I_{xx_{tot}}} \left[\left(I_{yy_{tot}} - I_{zz_{tot}} \right) \dot{\theta}\dot{\psi} - J_r \mathbf{\Omega}\dot{\theta} - d(L_2 - L_4) + \Sigma_{i=1}^4 (r_{i1}L_{i1} - r_{i2}L_{i2}) \sin \gamma_i \right] \ (40)$$

$$\ddot{\theta} = \frac{1}{I_{yy_{tot}}} \left[\left(I_{zz_{tot}} - I_{xx_{tot}} \right) \dot{\phi}\dot{\psi} + J_r \mathbf{\Omega}\dot{\phi} - d(L_1 - L_3) + \Sigma_{i=1}^4 (r_{i2}L_{i2} - r_{i1}L_{i1}) \cos \gamma_i \right] \ (41)$$

$$\ddot{\psi} = \frac{1}{I_{zz_{tot}}} \left[\left(I_{xx_{tot}} - I_{yy_{tot}} \right) \dot{\theta}\dot{\phi} - \Sigma_{i=1}^4 (MC_i + CDM_i) \right] \ (42)$$

where

$$I_{xx_{tot}} = I_{xx} + d^2\left(M_{S_2} + M_{S_4}\right) \ (43)$$

$$I_{yy_{tot}} = I_{yy} + d^2\left(M_{S_1} + M_{S_3}\right) \ (44)$$

$$I_{zz_{tot}} = I_{zz} + d^2\left(M_{S_1} + M_{S_2} + M_{S_3} + M_{S_4}\right) \ (45)$$

The parameter g represents the gravity. The parameters M_{STR}, M_{Si}, I_{xx}, I_{yy}, I_{zz}, J_r, d correspond to the quadrotor property of *ai2* at the *Universidad Politecnica de Valencia*. All the parameters used in this work are defined in Table 2. **L** and **Ω** represent the sum of the lift forces and rotational speeds, $\sum_{i=1}^4 L_{ij}$ and $\sum_{i=1}^4 |\Omega_i|$, respectively.

Table 2. Values of the parameters defining the bodies in VS-Lisp and parameters used in the simulations.

Parameter	Symbol	Value	Units
Structure Mass	M_{STR}	0.750	Kg
STR inertia around X_{STR} axe	I_{xx}	0.0081	Nms^2
STR inertia around Y_{STR} axe	I_{yy}	0.0081	Nms^2
STR inertia around Z_{STR} axe	I_{zz}	0.0016	Nms^2
Rotor Mass	M_{Si}	0.035	Kg
S_i rotational inertia around Z_{Si}	J_{ri}	6e-5	Nms^2
Blade length	l_{Bij}	0.07	m
Blade offset	e_{Bij}	0.05	-

Distance between STR_0 and S_{i0}	d	0.3	m

γ_i is the angular position in the rotor plane of the first blade and the parameter r_{ij} represents the application point of the lift force L_{ij} on the blade j of rotor i.

Equations (37)-(39) represent the linear acceleration of the structure's centre along X_n, Y_n and Z_n expressed in the structure based reference system. Equations (40)-(42) represent the angular accelerations around Y_{STR}, X_{STR} and Z_{STR} respectively.

This nonlinear model, obtained using VehicleSim modelling, is similar to that one obtained by (Palunko and Fierro, 2011) when the position of the vehicle's centre of gravity matches the centre of the structure and the rotors gyroscopic effect is not considered. Also (Martin and Salaun, 2010) obtained a model quite similar to the one obtained here that includes the rotors gyroscopic effect and the drag due to the vehicle's motion. However, none of these models consider the effect of having the aerodynamic forces applied at the blade's pressure center, represented by to the last terms appearing in equations (40) and (41).

Simulation results

With the equations of motion presented, including the control system and the trajectories generator, various simulations have been carried out in order to show the behaviour of the quadrotor's controlled model.

The simulations include both the rigid simple aerodynamic model and the elastic complete corrected aerodynamic model, described in Sections IV and V.

Figures 15 and 16 show a comparison of the achieved trajectories for these two models and the control actions that lead to that trajectory. As it can be seen, the trajectory tracking is similar for both models; however, the control actions that lead to these displacements are

very different. As expected, the elastic complete corrected model presents oscillations in the control actions in order to counteract the aerodynamic forces' oscillations; however, since the adaptive process is applied to the system, the amplitude of the oscillations is greatly reduced compared to the complete initial (non adaptive) elastic model case.
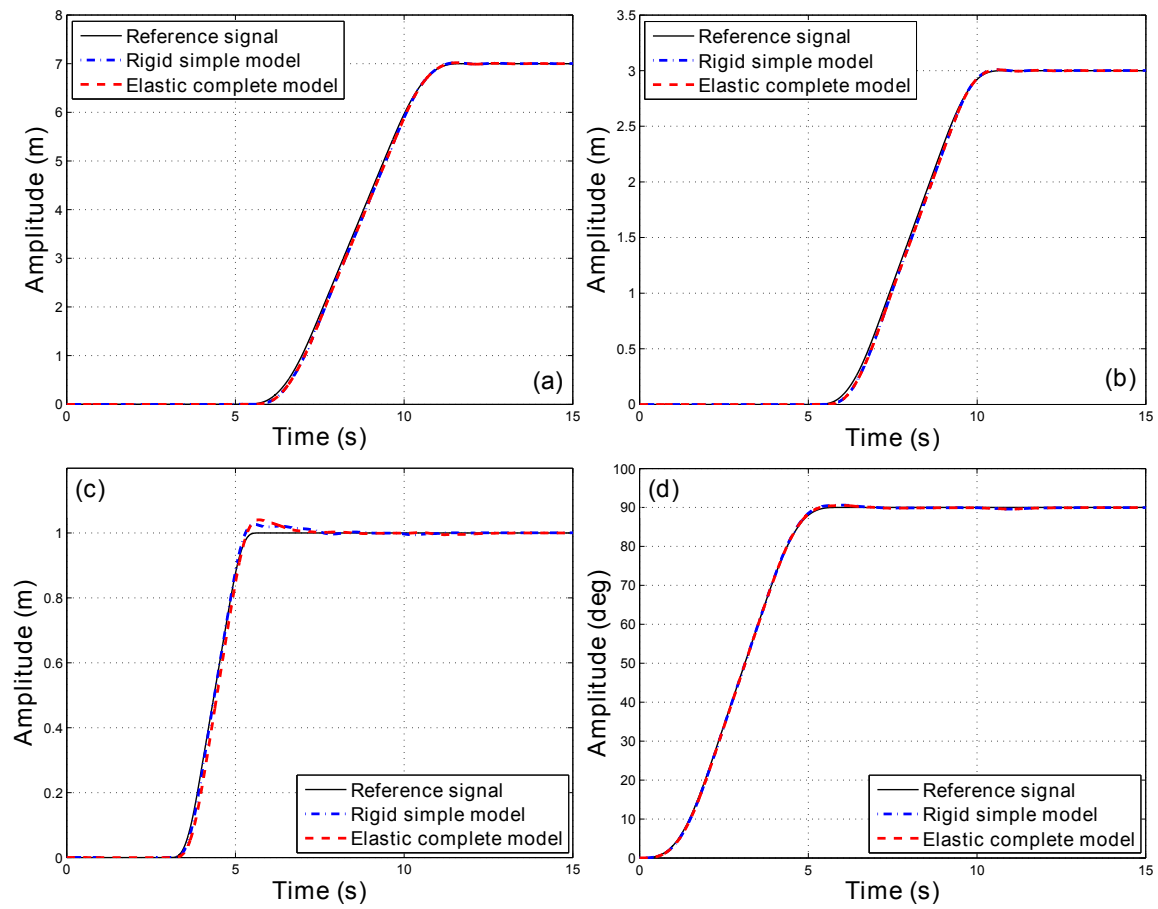

Figure 15. Example of quadrotor trajectories tracking for the different aerodynamic models. (a) X_n translation, (b) Y_n translation, (c) Z_n translation, (d) Z_{STR} yaw rotation .
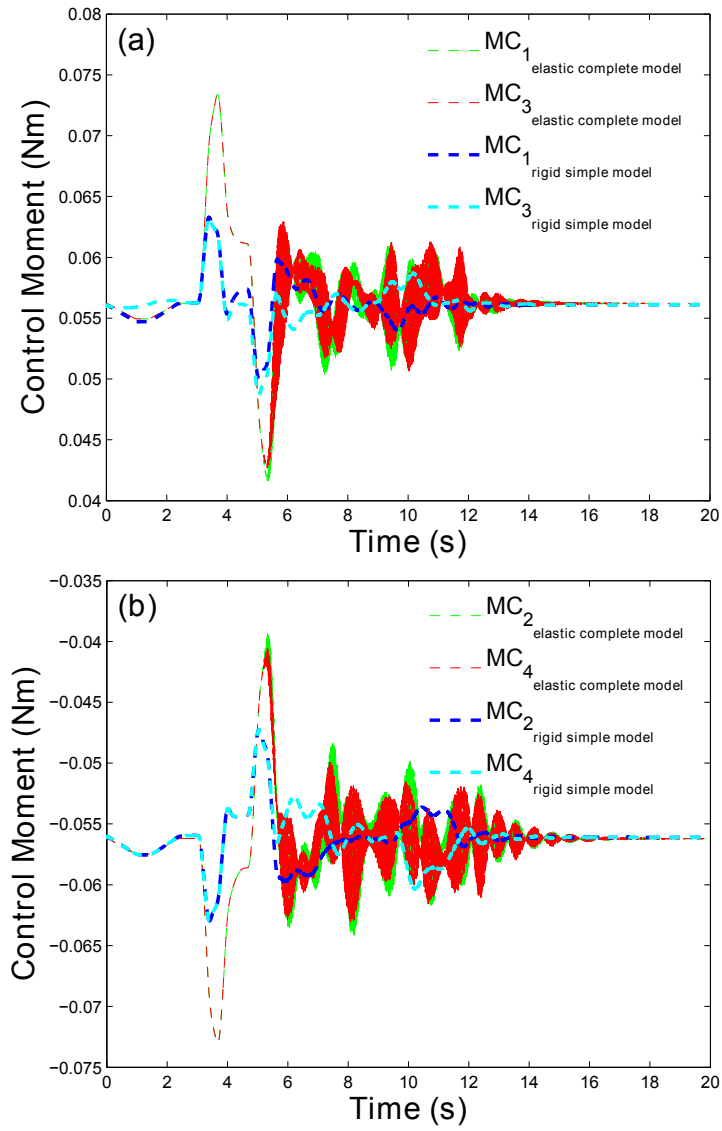
Figure 16. Control actions for achieving trajectories in Figure 15 for different models. (a) Control moment applied to rotors 1 and 3, (b) Control moment applied to rotors 2 and 4.

In Figure 16, it can be seen that in both cases the control actions are smaller than the maximum torque of the rotors, CM_{max} = 0.11 Nm.

Using the controlled model presented in (37)-(42) and the elastic complete corrected aerodynamic model ((13), (14), (36)), three-dimensional trajectories have been applied to the quadrotor. Figure 17 shows the simulation of a helicoidal trajectory of 3 meters radius and 50 meters height and Figure 18 represents the tracking of a rectangular trajectory of 10 meters side and 3 meters height.
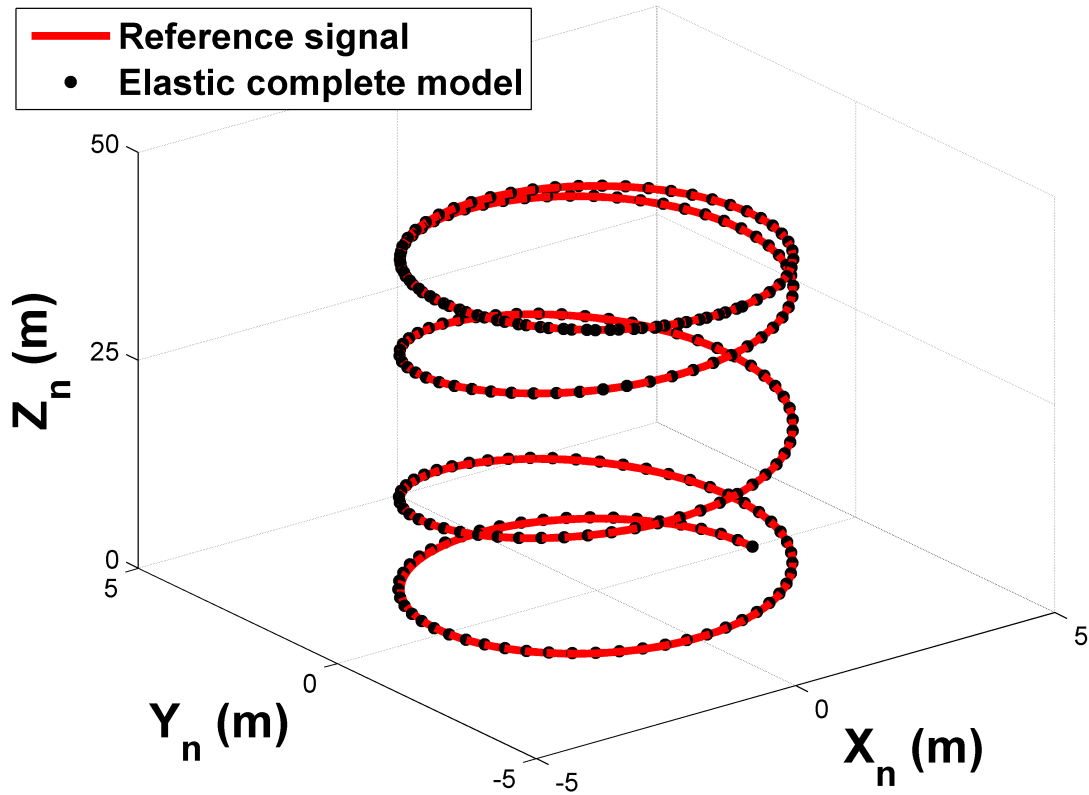
Figure 17. Three-dimensional helicoidal trajectory tracking using the elastic complete aerodynamic model. (---) is the reference signal and (*) is the elastic complete model trajectory.
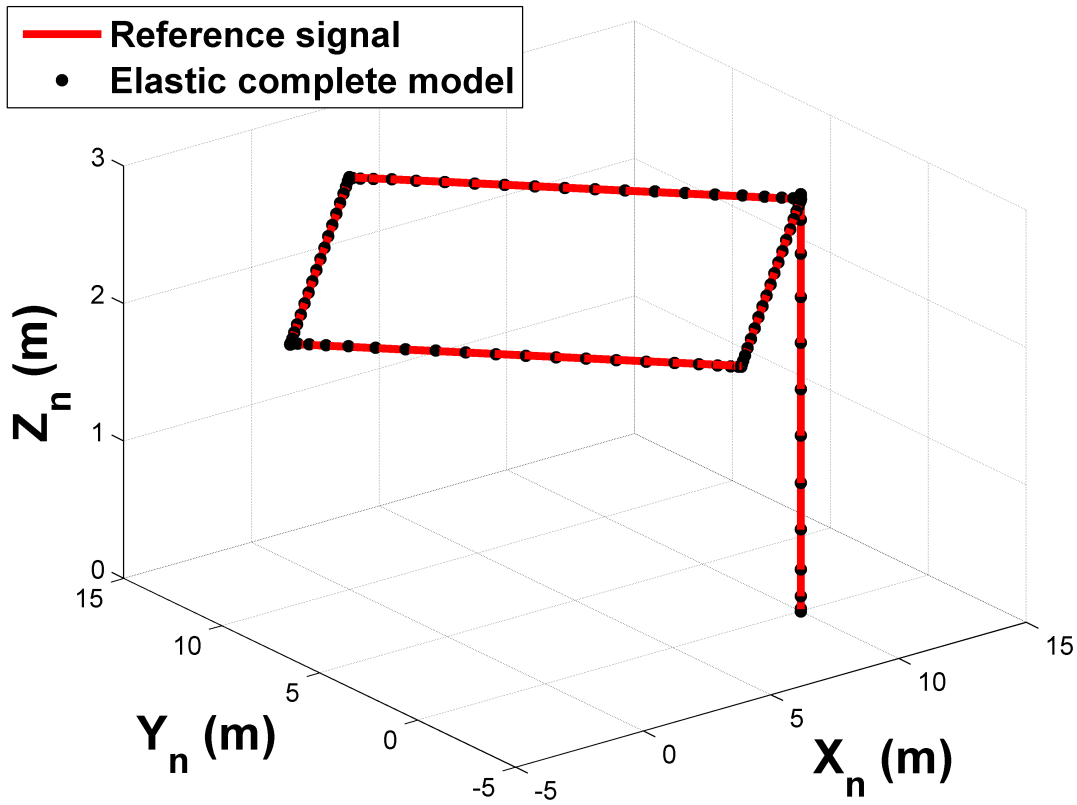

Figure 18. Three-dimensional rectangular trajectory tracking employing the elastic complete aerodynamic model. (---) is the reference signal and (*) is the elastic complete model trajectory.

In both cases, the quadrotor follows the prescribed trajectories satisfactorily.

Figures 19 and 20 show the control moments needed to achieve the motions represented in Figures 17 and 18 respectively.
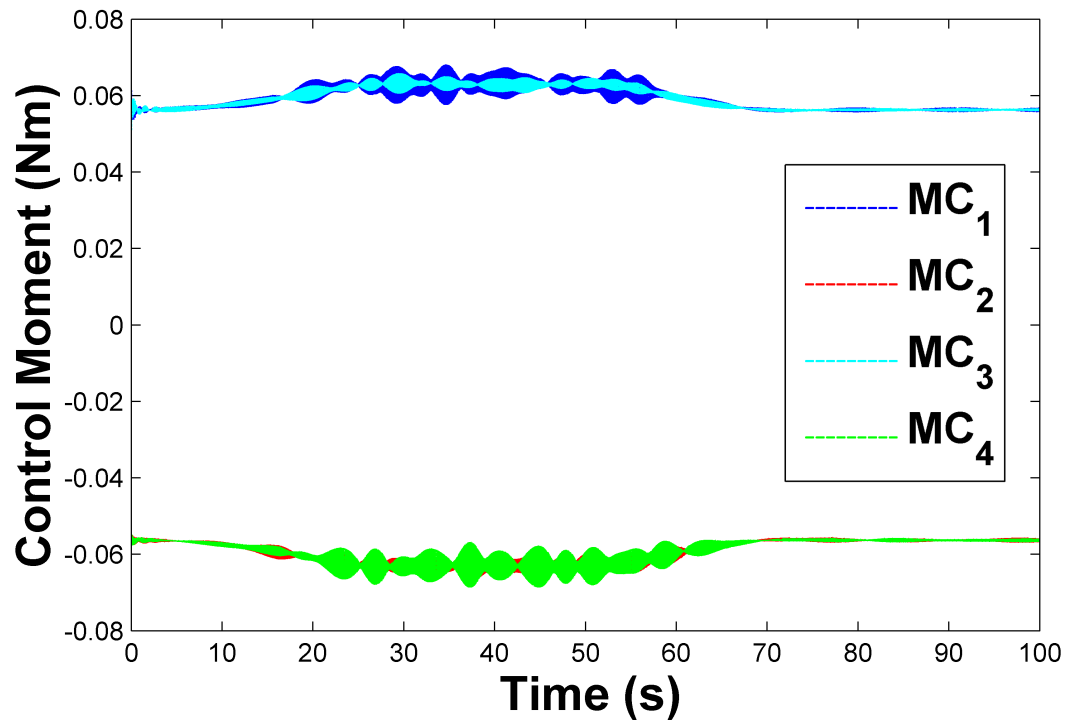

Figure 19. Control moments applied to obtain the three-dimensional helicoidal trajectory shown in Figure 17.
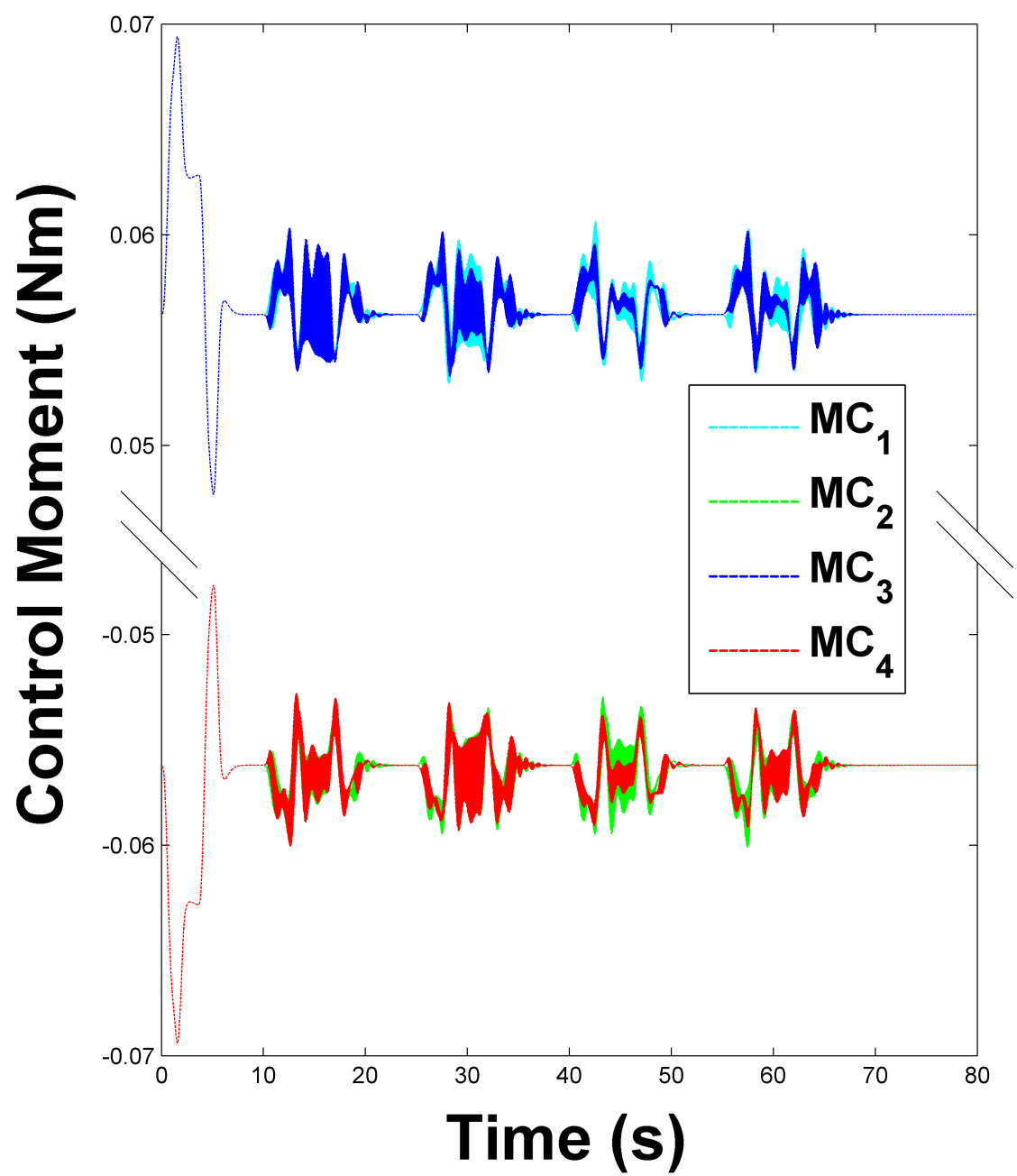
Figure 20. Control moments applied to obtain the three-dimensional rectangular trajectory shown in Figure 18.

As before, the control moments that produce the motion when the complete aerodynamic model is used, are of oscillating nature, but due to the smooth predefined trajectories and the adaptive methodology applied to the angular acceleration, they have a small amplitude, quite far from the maximum torque.

IX. Conclusions

In order to obtain a platform to study the vibrations appearing in quadrotors, an elastic quadrotor model, defined as a multibody system, has been designed and built using the multibody modelling software VehicleSim. A complete elastic bladed quadrotor model has been derived and full details on its implementation have been provided.

It has been proved to be an adequate software to derive the equations of motion of dynamical and mechanical systems, as shown in Section VIII, where the equations of quadrotor's motion provided by the software can be found.

Besides the structural models, various variable aerodynamic models have also been implemented by means of the Element Blade Theory and Prandtl's Lifting-Line Theory to calculate aerodynamic forces. One of the models only considers the rotational speed for the calculus of the aerodynamic forces, while the other one, more complex, also considers the effect of the translational speed on the aerodynamics and applies the forces at the pressure center of the blade, which differs from the vast majority of the works related to quadrotor's modelling until now.

A PVA linear control system has been used for the control of the vehicle's dynamics. The control structure - feedback of states - together with the smooth predefined trajectories,

allow to reach the desired trajectories with shorter response time, as well as shorter simulation time.

As a consequence of the consideration of the translational speed in the aerodynamics calculus, it is shown that oscillations appear in both, lift and drag forces. An adaptive process has been designed and presented to avoid the interference of these high amplitude oscillations in the control process, providing in this way a powerful tool to reduce the vibrations transmission to the control system.

The control system, together with the adaptive technique, has proved to be satisfactory when applied to both models, the simple aerodynamic model for which it was designed, and the elastic complete corrected aerodynamic model, that considers oscillating forces. The control method here used has been proven to be valid for the tracking three-dimensional trajectories and in the control of the drag moments and their effect on the rotational speed. This model represents in a way, a useful tool for control systems design and validation. The model here presented is nonlinear and it accurately captures the complex dynamics and couplings that in occasions are not taken into account when only linear approximations of the model are considered for control methods design purposes.

References

Alexis K, Nikolakopoulos G, and Tzes A (2012) Model predictive quadrotor control: attitude, altitude and position experimental studies. *Control Theory and Applications*, 6(12): 1812-1827.

Altas IH and Sharaf AM (2007) A generalized direct approach for designing fuzzy logic controllers in matlab/simulink gui environment. *International Journal of Information Technology and Intelligent Computing*, 1(4):1-27.

Anderson JDJ (2001) *Fundamentals of Aerodynamics*. Boston: McGraw-Hill Book Company.

Ashby MF (2005) *Materials selection in mechanical design*. Burlington MA: Butterworth-Heinemann.

Bouadi H, Cunha SS, Drouin A and Mora-Camino F (2011) Adaptive sliding mode control for quadrotor attitude stabilization and altitude tracking. In: *12th IEEE International symposium on computational intelligence and informatics*, Budapest, Hungary, 21-22 November 2011, pp. 449-455.

Bristeau PJ, Martin P, Salaun E, and Petit N (2009) The role of propeller aerodynamics in the model of a quadrotor uav. In: *Proceedings of the European Control Conference*, 2009, pp. 683-688.

Dundar, MA (2012) *Free vibration analyses of abs (acrylonitrilebutadiene-styrene) rectangular plates with completely free boundary conditions*. Thesis, Wayne State University, United States, 2012.

Erginer B and Altug E (2007) Modeling and pd control of a quadrotor vtol vehicle. In: *IEEE Intelligent Vehicles Symposium*, 2007, pp. 894-899.

Estelles S (2013) *Quadrotor Modelling and Control System Design*. MPhil Thesis, City University London, UK.

Evangelou SA, Limebeer DJN, Sharp RS and Smith MC (2006) Control of motorcycle steering instabilities. *Control Systems, IEEE*, 26(5): 78-88.

Evangelou SA, Limebeer DJN and Tomás-Rodríguez M (2008) Influence of Road Camber on Motorcycle Stability. *Journal of Applied Mechanics*, 75(6): 61020-61032.

Evangelou SA, Limebeer DJN and Tomás-Rodríguez M (2012) Suppression of burst oscillations in Racing motorcycles. *Journal of Applied Mechanics*, 80(1): 11003-11016.

Hajjaji E and Ouladsine M (2001) Modeling and nonlinear control of magnetic levitation systems. In: *IEEE Transactions on Industrial Electronics*, 2001, vol. 48, no. 4, pp. 831-838.

Hoffmann G, Huang H, Waslander SL, and Tomlin CJ (2007) Quadrotor helicopter flight dynamics and control: Theory and experiment. In: *AIAA Guidance, Navigation and Control Conference and Exhibit*, 2007, vol. 2.

Hoffmann G, Rajnarayan DG, Waslander SL, Dostal D, Jang JS, and Tomlin CJ (2004) The stanford testbed of autonomous rotorcraft for multi agent control (starmac). In: *Digital Avionics Systems Conference*, October 2004, vol. 2, pp. 12.E.4-1 -12.E.4-10.

Karden E, Buller S, Kok D, and Doncker RWD (2002) Modeling the dynamic behavior of supercapacitors using impedance spectroscopy: In: *IEEE Transactions on Industry Applications*, 2002, vol. 38, no. 6, pp. 1622-1626.

Kourosh P (2007) The lagrangian derivation of kane's equations. In: *Transactions of the Canadian Society for Mechanical Engineering*, October 2007, vol 31, pp. 407-420.

Limebeer DJN and Sharp RS (2006) Bicycles, motorcycles, and models. *Control Systems, IEEE*, 26(5): 34-61.

Le-Huy H (2001) Modeling and simulation of electrical drives using matlab simulink and power system blockset. In: *Annual Conference of the Industrial Electronic Society*, 2001, vol. 3, pp. 1603-1611.

Marichal GN, Tomás-Rodríguez M, Castillo Rivera S and Hernández López A (2012) Modelling and Analysis of Vibrations in a UAV Helicopter with a Vision System. *International Journal of Advanced Robotic Systems*, 9: 220

Marichal GN, Tomás-Rodríguez M, Hernández S, Castillo-Rivera S and Campoy P (2014) Vibration reduction for vision systems on board unmanned aerial vehicles using a neuro fuzzy controller. *Journal of Vibration and Control*, 20: 2243-2253.

Martin P and Salaun E (2010) The true role of accelerometer feedback in quadrotor control. In: *Robotics and Automation (ICRA), 2010 IEEE International Conference on*. Anchorage, Alaska, USA, 3-8 May 2010, pp. 1623-1629.

Mathworks (2014). Available at http://www.mathworks.co.uk/products/simulink (accessed on 14th November 2014).

McKerrow P (2004) Modelling the draganflyer four-rotor helicopter. In: *Proceedings of the IEEE International Conference on Robotics and Automation*, 2004, vol. 4, pp. 3596-3601.

Ning S and Bone GM (2002) High steady-state accuracy pneumatic servo positioning system with pva/pv control and friction compensation. In: *Proceedings of the International Conference on Robotics and Automation*, 2002, vol. 3, pp. 2824-2829.

Orban, F (2011) Damping of materials and members in structures. *Journal of Physics: Conference Series*, 268(1): 012-022.

Palunko I and Fierro R (2011) Adaptive feedback controller design and quadrotor modelling with dynamic changes of the center of gravity. In: *18th IFAC World Congress*, Milano, Italy, 28 August- 2 September 2011, pp. 2626-2631.

Park S, Won DH, Kang MS, Kim TJ, Lee HG and Kwon SJ (2005) RIC (Robust Internal loop Compensator) Based Flight Control of a Quad-Rotor Type UAV. In: *Intelligent Robots and Systems, 2005. (IROS 2005). 2005 IEEE/RSJ International Conference on*, August 2005.

Patel AR, Patel MA and Vyas DR (2012) Modeling and Analysis of Quadrotor using Sliding Mode Control. In: *44th IEEE Southeastern Symposium on System Theory*, Jacksonville, FL, USA, 11-13 March 2012, pp. 111-114.

Pivonka P and Miksnek V (2007) Real-time communication between matlab/ simulink and plc via process visualization interface. In: *Proceedings of the WSEAS International Conference on Systems*, 2007, vol. 2, pp. 28-32.

Qiu A, Wu B, and Kojori H (2004) Sensorless control of permanent magnet synchronous motor using extended kalman filter. In: *Canadian Conference On Electrical and Computering Engineering*, 2004, vol. 3, pp. 1557-1562.

Ramirez CM, García-Fernández P, De-Juan A and Tomás-Rodríguez M (2013) Interconnected Suspension System on Sport Motorcycle. In: *Proceedings of the 2nd Conference MeTrApp*, vol. 17, pp. 9-16.

Ramirez CM and Tomás-Rodríguez M (2014) Non linear optimization of a sport motorcycle's suspension interconnection system. In: *2014 UKACC International Conference on Control*, July 2014, pp. 319-324.

Ramirez CM, Tomás-Rodríguez M and Evangelou SA (2012) Dynamical analysis of a duolever suspension system. In: *2012 UKACC International Conference on Control*, Sept. 2012, pp. 1106-1111.

Ropp ME and Gonzalez S (2009) Development of a matlab/simulink model of a single-phase grid-connected photovoltaic system. In: *IEEE Transactions on Energy Conversion*, 2009, vol. 24, no. 1, pp. 195-202.

Salih AL, Moghavvemi M, Mohamed AF and Gaeid KS (2010) Modelling and PID Controller Design for a Quadrotor Unmanned Air Vehicle. In: Automation Quality and Testing Robotics (AQTR), 2010 IEEE International Conference on, May 2010, vol. 1, pp. 1-5.

Tomás-Rodríguez M and Sharp R (2007) Automated modeling of rotorcraft dynamics with special reference to autosim. In: *IEEE International Conference Automation Science and Engineering*, pp. 974-979.

VehicleSim. Available at http://www.carsim.com/ (accessed on 14th November 2014).

Venkatesan C (2014) *Fundamentals of helicopter dynamics*. CRC Press.